RSC Advances

This is an *Accepted Manuscript*, which has been through the Royal Society of Chemistry peer review process and has been accepted for publication.

Accepted Manuscripts are published online shortly after acceptance, before technical editing, formatting and proof reading. Using this free service, authors can make their results available to the community, in citable form, before we publish the edited article. This *Accepted Manuscript* will be replaced by the edited, formatted and paginated article as soon as this is available.

You can find more information about *Accepted Manuscripts* in the Information for Authors.

Please note that technical editing may introduce minor changes to the text and/or graphics, which may alter content. The journal's standard Terms & Conditions and the Ethical guidelines still apply. In no event shall the Royal Society of Chemistry be held responsible for any errors or omissions in this *Accepted Manuscript* or any consequences arising from the use of any information it contains.

ROYAL SOCIETY OF CHEMISTRY

www.rsc.org/advances

Triboelectric Generator Composed of Bulk Poly(vinylidene fluoride) and Polyethylene Polymers for Mechanical Energy Conversion

Piyush Kanti Sarkar,[a] *Subrata Maji,*[a] *Gundam Sandeep Kumar,*[a] *Krushna Chandra Sahoo,*[a] *Dipankar Mandal* [b] *and Somobrata Acharya**[a]

[a]Centre for Advanced Materials (CAM), Indian Association for the Cultivation of Science, Jadavpur, Kolkata 700032, India.

[b]Department of Physics, Jadavpur University, Kolkata 700032, India.

*Corresponding author E-mail: camsa2@iacs.res.in

Abstract: We designed a stable triboelectric generator (TEG) consisting of new combination of poly(vinylidene fluoride) (PVDF) and polyethylene (PE) films which shows prospect for easy and low cost device fabrication. Both PE and PVDF are selected from negative side of triboelectric series considering the difference in charge affinity. An open circuit peak-to-peak output voltage of ~20 V and current density ~0.34 Am^{-2} was obtained just by striking the TEG manually. The effect of directional forces on TEG was studied for futuristic pressure anisotropic sensor fabrications. The charging capacity of TEG was checked by using a commercially available capacitor revealing the prospect of battery charging. Furthermore, the TEG powered at least 12 commercial white light emitting diodes which indicate a potential use as carbon emission free power source suitable in portable electronic devices.

Keywords: Energy conversion, polyethylene, PVDF, triboelectricity, triboelectric generator.

RSC Advances Accepted Manuscript

INTRODUCTION

Unconventional energy harvesting technologies are of great interest in renewable and green energy application area. In this regards, different types of energy generation mechanisms have been adopted including photoelectric effect,[1-5] vibration energy harvesting,[6,7] thermoelectric conversion,[8-10] piezoelectric phenomena[11-15] and the triboelectric effect.[16-18] Out of these, piezoelectric and triboelectric energy generation from polymer based materials have received increasing interest recently because of their flexible, durable, and light weight properties. Being mechanical energy harvesting systems, these generators are effective and promising to use as a self-powered electronic devices, touch sensors and electronic skin.[19-22] Piezoelectric generators are based on the materials, that have the ability to transform applied mechanical strain into electric potential via change in dipole moments.[11] On the other hand, triboelectric generator (TEG) response is based on the transfer of electrons from one material to another when two materials with different charge affinity come into contact and then separate.[16] This simple working principle makes the TEG relatively cost-effective and largely scalable in comparison to the piezoelectric generators for mechanical energy harvesting since the materials for TEG are largely abundant. Hence, the central focus is to generate energy using tribo-electrification to boost up the output power for effective power source for practical applications. In addition, the output power from piezoelectric generator often combines the contribution of both piezoelectric and triboelectric effects. For example if triboelectric effect occurs within a piezoelectric generator due to friction between the active piezoelectric materials. Similarly in a TEG, piezoelectricity can affect the resulting charge generation if a piezoelectric material is used in the device fabrication. Hence, fundamentally it is important to separate the effect of triboelectricity and piezoelectricity within a mechanical power generator device.

RSC Advances Accepted Manuscript

In this work, we report on the fabrication of triboelectric generator using the combinations of two cost-effective polymers, namely, poly(vinylidene fluoride) (PVDF) and polyethylene (PE). For fabricating triboelectric generator, active materials are usually chosen from positive and negative sides of triboelectric series.[16,22-24] However, both PE and PVDF are selected from negative side of triboelectric series considering their difference in charge affinity and to testify the device efficiency when materials combinations in TEG are chosen from the negative side of triboelectric series. Since PVDF is a well-known piezoelectric material,[19,25] we have fabricated the device structure is such a way that only one surface of the PVDF film remains connected to the electrode. Hence, the effect of piezoelectricity within the triboelectric generator can be avoided since piezoelectricity occurs only when both the surface of the film is connected to electrodes. We have also tested the effects of directional forces in TEG that attributes to potential use as anisotropic pressure sensors applications along with the harvesting mechanical energy. We have obtained peak-to-peak output voltages of ~20 V with an output short circuit current of ~31 μA from the TEG under vertically applied forces that promises to the wide range applications to directly power up several tiny portable electronic gadgets. Furthermore, our TEG can differentiate the weight differences of coins, which enables it to be used as a self-powered pressure sensor.

EXPERIMENTAL DETAILS

Fabrication: TEG was fabricated in sandwich pattern using two rectangular steel plates (0.8 mm thick) as top and bottom electrodes. PE tape was first attached to one steel electrode. PVDF solution was prepared by mixing 1g of PVDF pallets (Sigma-Aldrich, USA) with 4 ml dimethylformamide (DMF). The solution was stirred at 60 °C for 4 h. Then 4 ml acetone was

RSC Advances Accepted Manuscript

mixed to it and stirred at room temperature. PVDF film was fabricated on top of another steel electrode by drop cast method from resulting PVDF solution. Afterwards, the PVDF-steel electrode was annealed for an hour at 60 °C under nitrogen environment. The thickness of PE and PVDF film was ~0.14 mm and ~15 µm respectively. We ensured that the PVDF film was continuous and fully attached to the electrode. In the next step, PE-steel electrode and the PVDF-steel electrodes were stacked together in form of a sandwich pattern device with an effective area of 9 cm^2 (figure 1a). A thick elastic tape lock at one edge of the device is attached so that PVDF and PE remain separated (X_{max}, maximum separation is 4 mm) in absence of any external force (figure 1b). For electrospun PVDF based TEG, the electrospinning of the PVDF is employed by horizontal electrospinning method. The solution of PVDF was loaded into a syringe fitted with a metallic needle and kept at 15 cm away from the steel electrode collector. Electrospinning was performed by employing a high voltage of 15 kV with the feed rate of 1 ml/h.

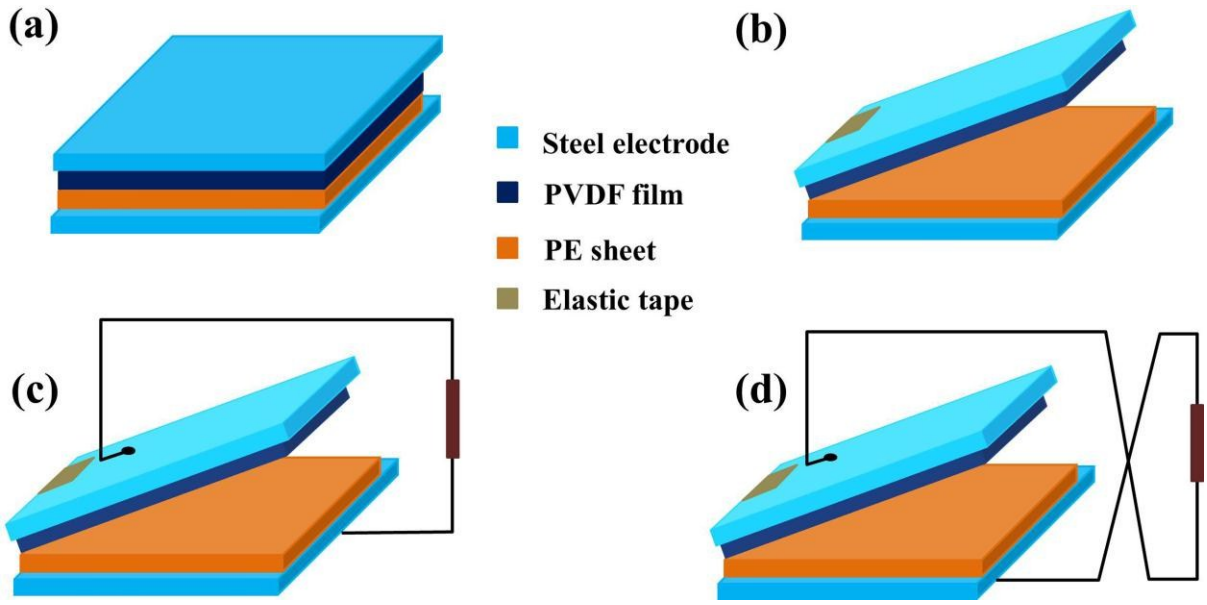

Figure 1. (a) Schematic structure of the TEG layer by layer. (b) Schematic of the TEG after attaching the tape to separate the polymer materials when no mechanical force is applied. (c) Forward connection and (d) Reverse connection of the TEG to the oscilloscope.

RSC Advances Accepted Manuscript

Measurements: Output voltage from the device under periodic external forces was measured by a digital oscilloscope (Yokogawa DL1620). Output current of the device was measure by Keysight B2987A picoammeter. Periodic force was applied manually with a wooden piece. When the positive probe of the oscilloscope was connected to the PVDF-steel electrode and the ground was connected to the PE-steel electrode, it was treated as the forward connection (FC), (figure 1c). The inverted connection was defined as the reverse connection (RC), as shown in figure 1d.

RESULTS AND DISCUSSION

The mechanism of the output voltage generation is schematically shown in figure 2. When the electrodes are separated from each other, the device remains in equilibrium state (Figure 2a). Upon applying the first striking force to the device, PVDF and PE films touch and rub against each other. This generates electrostatic charges with opposite signs, which are distributed on the surface of two polymer films. In this case, PVDF becomes negatively charged and PE becomes positively charged according to the triboelectric series (Figure 2b).[26] However, at

RSC Advances Accepted Manuscript

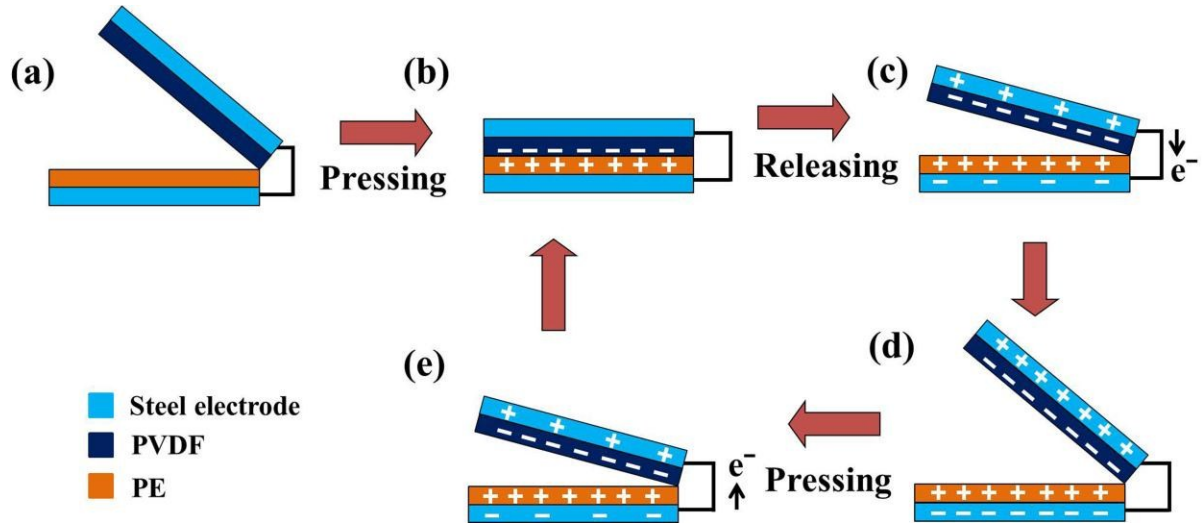

Figure 2. Mechanism of the TEG when pressed and released. (a) The device at rest before applying any forces. No charges are built up on the surfaces of the polymers. (b) Charge distribution in the device after first striking. At this point, no charges have been induced on the electrodes as the negative charges on PVDF surface and the positive charges on PE surface are close to each other. (c) Induction of the charges on the electrodes and flow of charges through external load while the device is being released and the distance between the two polymer surfaces is increasing. (d) Electrostatic equilibrium state when the electrodes are fully induced. (e) Charge distribution and charge flowing direction when the distance between the electrodes is decreasing while the external force is withdrawn.

this point, these charges will not induce any charges on the electrodes since the positive and negative charges are situated close to each other. Just after the striking, the device relaxes owing to the flexibility induced by the attached thick elastic tape. During the process, the polymer films are separated from each other inducing static charges on the counter electrodes. Negatively charged PVDF film will induce positive charges on the electrode attached to it at the near end. Similarly, positively charged PE film will induce negative charges on the electrode attached to it at the near end. In this configuration, the counter charges located at the far ends of the electrodes will move to the opposite electrodes making these more positive and negative in nature (Figure

RSC Advances Accepted Manuscript

2c). This process induces the flow of free electrons through the external load generating negative peak for FC. The current will continue till induced charges flow to the electrodes (Figure 2d). However, the charges on both the polymer surfaces remain static owing to the insulating nature of PVDF and PE. After applying the next striking force, the electrodes approach into closer proximity (Figure 2e) and finally touch each other mimicking previous structure as on figure 2b. While the separation between the two polymers is decreasing, positively charged PE will repel the induced positive charges on the electrode attached to PVDF. This will create flow of free electrons towards the PVDF-electrode generating a positive peak for FC. Current will continue till the two polymers come in contact with each other and charges are neutralized from the electrodes (Figure 2b). These cycles continue repetitively with the applied periodic forces.

In order to investigate the output performance of the TEG, periodic forces were applied manually on the device from different directions. The output signals from TEG for the vertically applied forces are shown in figure 3. An open circuit peak-to-peak output voltage of ~20 V (Figure 3a) and short circuit current of ~31 μA (Figure 3b) was obtained in FC mode. The absolute value of the short circuit transferred charges (Q_{sc}) in a half cycle was found to be 0.0267 μC (calculated by integrating a single current peak in half cycle). We reversed the connection (RC mode) to verify the actual output from the TEG and its consistency. Similar output characteristics (Figure 3c, 3d) were obtained from the TEG in RC mode as well. For further clarification of the output characteristics, the output characteristics from the two electrodes were simultaneously connected to two channels of a digital oscilloscope, the corresponding results are shown in figure 3e. The enlarged image of one peak of figure 3e is presented in figure 3f, which shows the signals from two electrodes are exactly opposite to each other. Additionally, we have measured the Fourier transform infrared spectroscopy (FTIR) of the drop casted PVDF (Figure

RSC Advances Accepted Manuscript

4a and 4b). The strong peaks at 766 cm^{-1} and 795 cm^{-1} indicate the presence of α-phase in the film, whereas the presence of β and γ-phases are assigned from the peaks at 1279 cm^{-1} and 1233 cm^{-1}.[25] To quantify the relative proportion of electroactive β and γ-phases, we have deconvoluted the FTIR spectra (915-760 cm^{-1} regions). Absorption intensity at

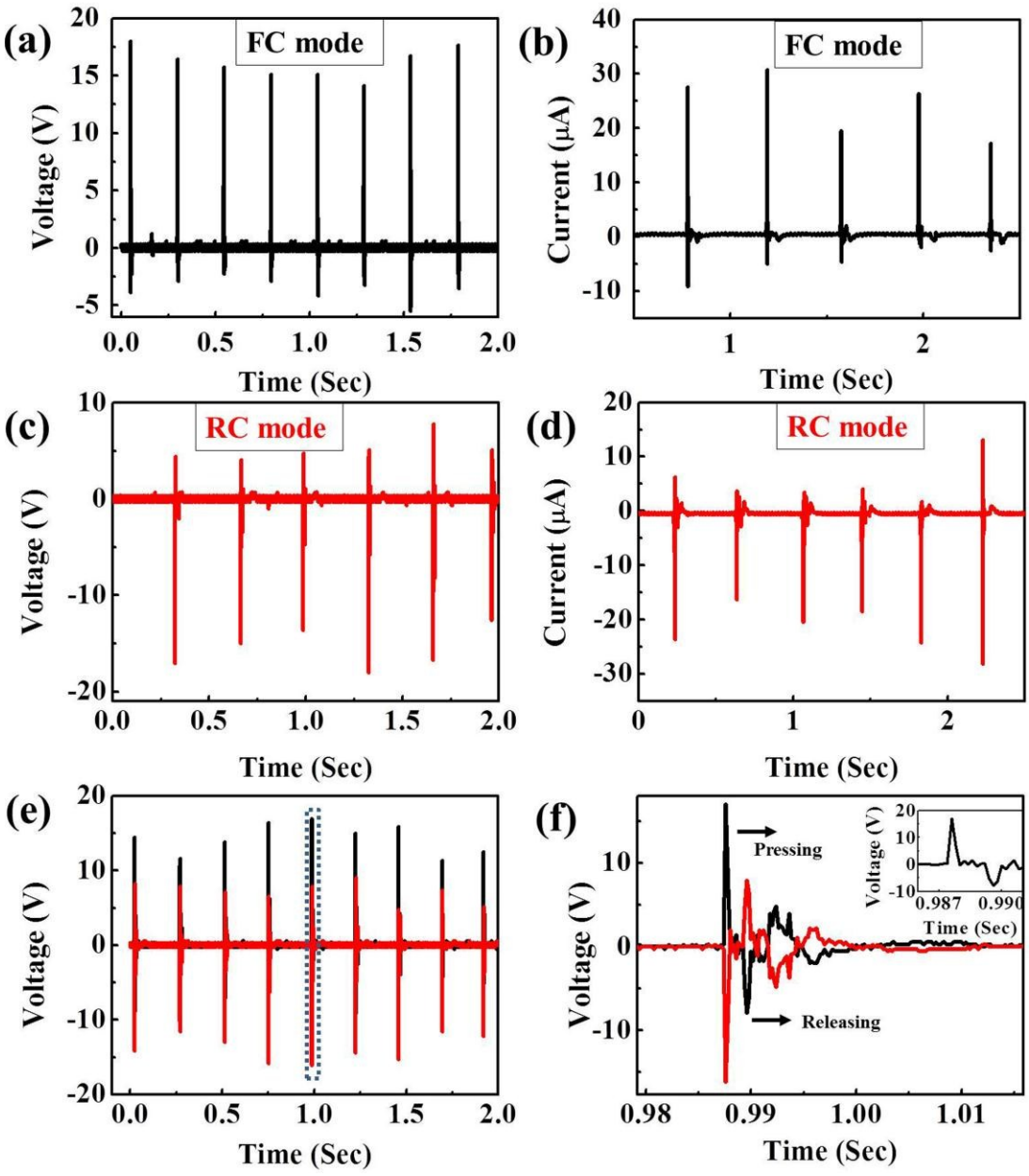

RSC Advances Accepted Manuscript

Figure 3. Output voltages and currents of the TEG under a periodic force applied through a wooden piece by hand. (a) Output voltage of the TEG for forward connection (FC), (b) Short circuit current of the TEG for FC, (c) Output voltage of the TEG for reverse connection (RC), (d) Short circuit current of the TEG for RC, (e) Output voltage from the two electrodes simultaneously, (f) Zoomed image of one peak of figure 3e, position of the peak for pressing and releasing is shown for the black curve, i.e., for the FC. Inset shows zoomed picture of first peak of black curve in figure 3f.

840 cm^{-1} conveys dual characteristics of both β and γ-electroactive phases (F_{EA}). The relative proportion of electroactive phases (F_{EA}) attributed to both β and γ-phases can be calculated using the following equation:

$$F_{EA} = \frac{I_{EA}}{\left(\frac{K_{840}}{K_{766}}\right) I_{766} + I_{EA}} \times 100 \quad (1)$$

where, I_{766} and I_{EA} are the absorbance intensity at 766 cm^{-1} and 840 cm^{-1}, respectively; K_{766} and K_{840} are the absorption coefficient at the respective wavenumbers.[27] From the deconvoluted curve (Figure 4b), calculated electroactive phase (F_{EA}) is found to be 60%. The individual β and γ-phases are calculated by curve deconvolution of the 840 cm^{-1} band, where the broadening contribution due to γ-phase and the sharp, well resolved peak for β-phase have been considered.

RSC Advances Accepted Manuscript

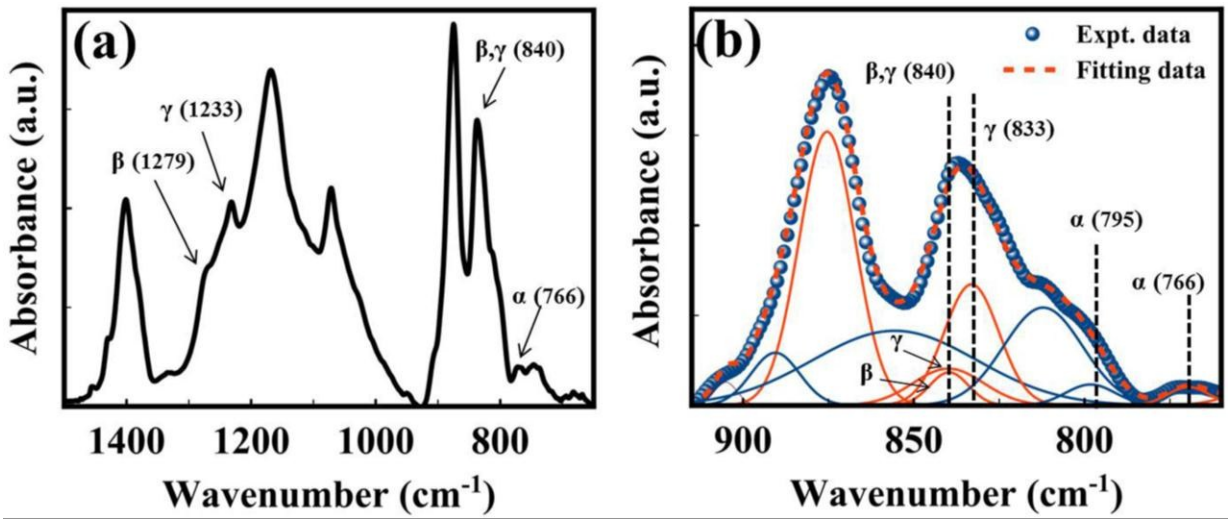

Figure 4. (a) FTIR spectrum of drop casted PVDF film. (b) Deconvoluted FTIR spectra (915-760 cm^{-1}) of drop casted PVDF film. Corresponding PVDF phases are marked in the figure.

The following equations are used to quantify the relative proportion of electroactive β and γ-phases individually.[25]

$$F(\beta) = F_{EA} \times \frac{A_\beta}{A_\beta + A_\gamma} \times 100 \quad (2a)$$

$$F(\gamma) = F_{EA} \times \frac{A_\gamma}{A_\beta + A_\gamma} \times 100 \quad (2b)$$

Where, A_β and A_γ are the integrated areas under the β and γ-marked deconvoluted curves in figure 3d centered at the 840 cm^{-1} band. The individual $F(\beta)$ and $F(\gamma)$ are found to be ~20% and ~40% respectively. This indicates that the contribution from γ-phase to the relative proportion of electroactive phases (F_{EA}) is higher than the contribution from β-phase. The lower proportion of β-phase suggests that the output response is not coming from piezoelectricity of PVDF film.

RSC Advances Accepted Manuscript

Additionally, the introduction of PE film within the TEG rule out any output voltage that may have originates from piezoelectricity. These observations support the fact that the output signals of the TEG arise due to triboelectric effect only.

The role of rough surfaces to generate more surface charges during friction for enhanced triboelectric effect was demonstrated earlier.[24] Surface morphologies of the drop casted PVDF film and PE tape were studied using Scanning Electron Microscope (SEM) (figure 5a and 5b). Randomly distributed fibril structures in each spherulites forming a rough surface are observed in the drop casted PVDF film. Such surface roughness is beneficial for the TEG device performance. In comparison to the PVDF film, the surface morphology of polyethylene film appears relatively smooth (figure 5b, for example, red marked regions). Hence, few scratches were made manually on the surface of the PE film to induce surface roughness which is supposed to increase the friction between PVDF and PE film within the TEG. For further investigation on the effect of film roughness on the TEG device performance, we have prepared TEG consisting of electrospun PVDF fibers instead of drop casted PVDF film. Surface morphology of the electrospun PVDF film was studied in SEM (Figure 5c). The output voltages of the TEGs consisting of smooth PE, scratched PE and electrospun PVDF (with scratched PE) film are compared in Figure 5d. Maximum peak-to-peak output voltage for TEG consisting of smooth PE and drop casted PVDF is found to be ~12 V which is much lower than that of TEG consisting

RSC Advances Accepted Manuscript

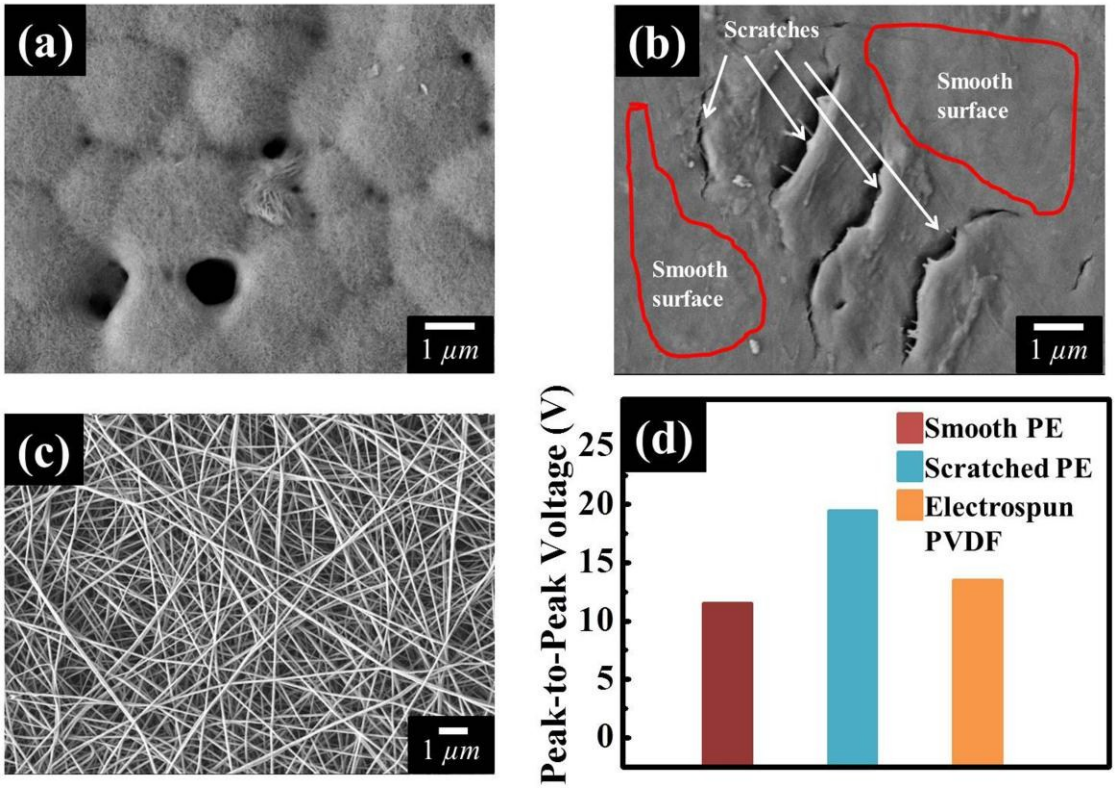

Figure 5. FE-SEM images of (a) drop casted PVDF film and (b) polyethylene tape. Scratches are shown by white arrows and red loops show the smooth surfaces. (c) SEM image of the electrospun PVDF and (d) Comparison of output voltages from different TEGs consisting of smooth PE, scratched PE and electrospun PVDF respectively.

of scratched PE and drop casted PVDF. Maximum peak-to-peak output voltage for the electrospun PVDF and scratched PE based TEG is found to be ~14 V which is relatively lower than the output voltage of the drop cast PVDF based TEG. Lower output voltage for the electrospun PVDF based TEG in comparison to the drop cast PVDF based TEG may be attributed to the lower effective contact area of electrospun PVDF fibers with PE film and its poor adhesion with steel electrodes, especially as per adopted device geometry is concerned.

RSC Advances Accepted Manuscript

To study the effect of directionality of hammering forces, we used the TEG without the thick elastic tape which was used previously for electrode separation. We have applied the forces in ~40° and ~60° angles on the upper steel electrode so that the electrode along with the PVDF film slides a little on the PE film and causes separation of charges. The results were compared with that of the TEG with vertical forces (90°). Schematic for applied forces from different directions and their effect on output voltages are given in figure 6. Figure 6d shows the output voltage for the applied sliding forces on the upper electrode with ~40° angle as shown in figure 6a. Figure 6e shows the output voltage for the same system under the sliding force with a higher angle ~60°. Corresponding schematic diagram is shown in figure 6b. Figure 6f shows the output voltage of the TEG under vertical forces, which is perpendicular to the top electrode (Figure 6c). When the direction of applied force is the lowest (Figure 6a), the output voltage is found to be the lowest in

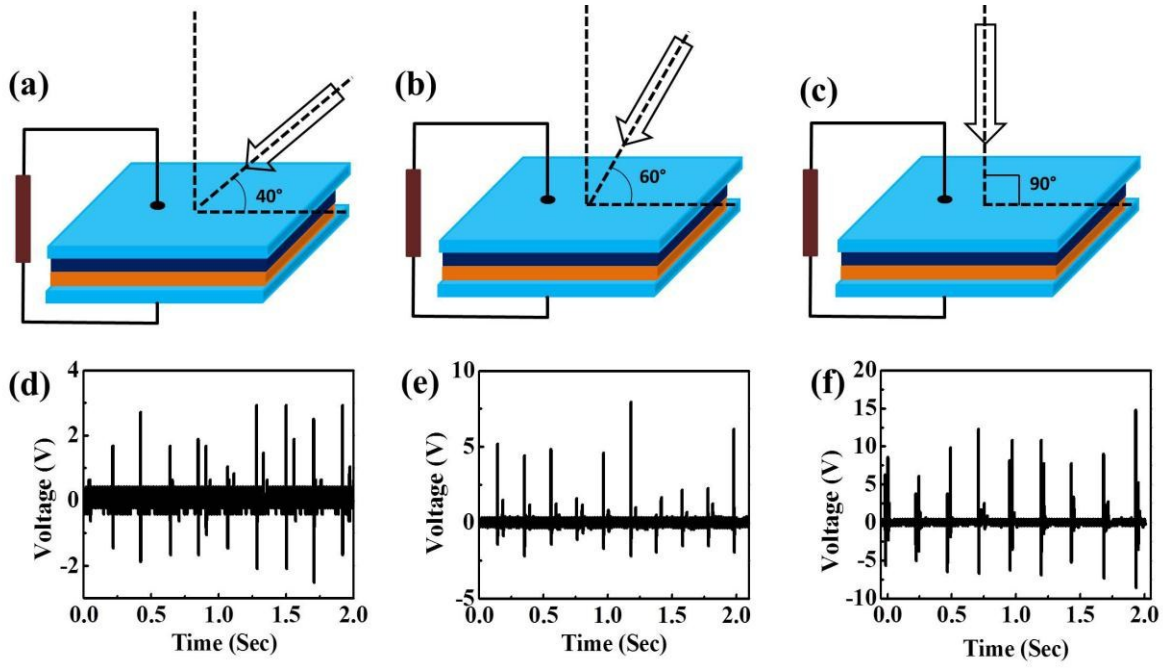

RSC Advances Accepted Manuscript

Figure 6. Schematic diagram for different types of forces on the TEG with no thick elastic tape attached. Sliding force is applied on the upper electrode at ~40° angle (a) and at 60° angle. (c) Vertical force (90° angle) is applied on the upper electrode. Output voltage for the TEG, when no thick elastic tape is used, with sliding forces at ~40° (d) and at ~60° (e). (f) Output voltage for the TEG under vertical forces.

comparison to other two directions. This observation clearly shows that the output voltage increases with increasing the striking angle with respect to the top electrode. This is due to the fact that when the sliding of the top electrode occurs, negative charges are accumulated on PVDF surface and positive charges will be generated on PE surface. Since sliding of the surfaces takes relatively longer time, the charges generated on two polymer surfaces will not be separated immediately. As a result, the possibility of recombination of negative charges on PVDF with the positive charges on PE will increase resulting in lower output voltage. When the striking angle is increased (Figure 6b), the sliding occurs for lesser time diminishing the possibility of charge recombination, thus increasing the output voltage. For vertical forces, the polymers come to contact for a little period of time and polymers are separated immediately after the strike. As a result, the charges on the surfaces of two polymers have lesser possibility of recombination resulting in higher output voltage. The process is reinforced by the use of thick elastic tape (Figure 1b) in the TEG, which helps the polymers to be separated immediately after applying the vertical force enabling efficient in energy generation.

For application of the TEG as a power source, the effective electric power generation is estimated by connecting different resistors as external load.[19] Output currents and power outputs ($W= I^2_{peak}R$) are plotted for different load resistances (Figure 7a). The current decreases with increasing load resistance due to ohmic loss.[24] Maximum instantaneous output power reaches to

RSC Advances Accepted Manuscript

160 μW for 900 kΩ of load resistance with power density 0.178 Wm^{-2} signifying that our TEG is quite efficient for the particular load resistance. To show the practical implementation of our

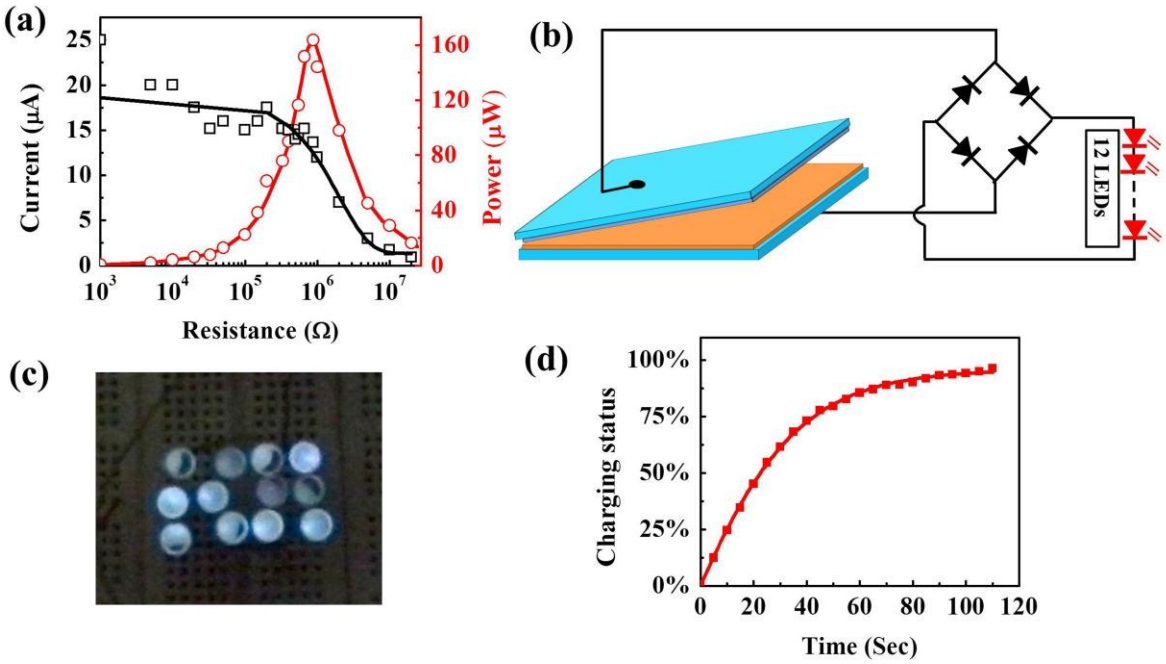

Figure 7. (a) Current versus resistance (black curve) and output power versus resistance (red curve). (b) Schematic of the TEG and circuit diagram for powering the LEDs. (c) Snapshot of powering LEDs from TEG by applying periodic vertical forces. (d) Transient response of the capacitor, when connected with the TEG through a bridge rectifier.

TEG, we have connected few commercial white light emitting diodes (LEDs) with the TEG using a typical bridge rectifier circuit (Figure 7b). It was able to power up at least 12 white LEDs intensely by simply tapping with hand, the concerning snapshot provided in figure 7c (electronic supplementary information, Video S1). This clearly illuminated the bread broad where even individual connecting holes were also clearly visible, indicating to use as an effective energy harvesting power source for decorating with LEDs and illuminating the roads where the mechanical stimuli can be directly utilized from the environment. The charging capacity of TEG

RSC Advances Accepted Manuscript

was checked by connecting a commercial capacitor (2.2 μF) though a bridge rectifier and striking the TEG at 3 Hz of frequency and subsequently measured the voltage across the capacitor. The transient response of capacitor charging is shown in figure 7d. This implies that the energy of the TEG can be stored by charging a battery for further use.

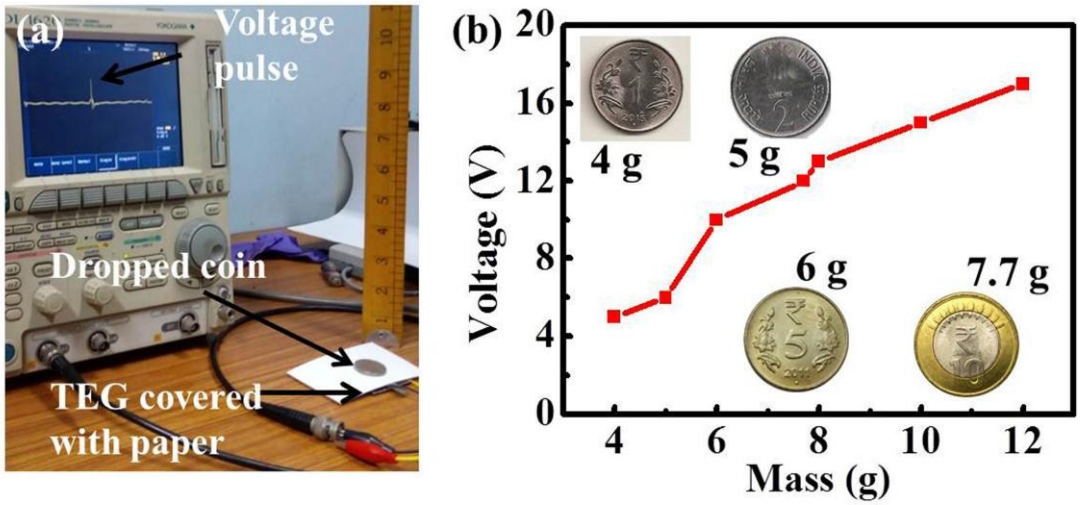

Figure 8. Illustration of the TEG used as a self-powered pressure sensor. (a) Setup image of the coin drop test. Coins of different mass are dropped from a height of about 15 cm on the TEG. Instant response can be seen from the voltage peak in the image. (b) The peak voltage response for various types of coins. Inset shows the picture of different types of coins used.

Our TEG showed potential to be used as a self-powered pressure sensor as it generates voltage or current through contact electrification between two triboelectric materials by external mechanical force. To illustrate this capability, some standard Indian coins carrying different weights were dropped from a fixed height to the central area of the TEG. The TEG was covered with a paper piece to avoid any charge flow upon contact between coins and electrode. When a coin drops on the TEG, PVDF and PE come into contact with each other, leading to a detectable signal output. Figure 8 illustrates the coin drop test for application of the TEG as a self-powered pressure sensor. Different types of coins (1 rupee, 2 rupee, 5 rupee and 10 rupee) were used and

RSC Advances Accepted Manuscript

dropped from a height of ~15 cm on the central area of the TEG. The peak voltage response for various types of coin with different masses is plotted in figure 8b. Expectedly, the heaviest coin generates the maximum output voltage.

CONCLUSIONS

In summary, we developed a very simple method to fabricate a stable triboelectric generator consisting of PVDF and PE films. We are able to rule out the piezoelectricity effect, which may originate from PVDF film/electrospun fibers within the TEG by introducing PE films within the device geometry. The TEG shows prospect of easy and low cost device fabrication with high electrical output performance. Furthermore, the effect of directional forces on TEG is studied for verifying the harvesting mechanical energy capability and also futuristic pressure anisotropic sensor fabrications. The TEG gives open circuit peak-to-peak output voltage of ~20 V and maximum short circuit current of ~31 μA with current density ~0.34 Am^{-2} just by striking the TEG manually with a wooden piece. Moreover, the TEG is able to power at least 12 commercially white LEDs directly just by tapping with hand indicating a potential use as carbon emission free power source suitable in portable electronic devices, lighting the roads, transportation monitoring and so on. Furthermore, The TEG is used to differentiate the mass of different coins. This study opens up the possibility of the TENG to utilize in self-powered power sensor. The easy fabrication of TEG consisting of a new combination of polymers may add an additional benefit for batch fabrication and easy commercialization.

RSC Advances Accepted Manuscript

ACKNOWLEDGEMENTS

Financial support from SERB (EMR/2014/000664), DST, India is gratefully acknowledged. P. K. S. and G. S. K. gratefully acknowledge the DST-INSPIRE fellowship. S. M. and K. C. S. gratefully acknowledge CSIR, India for fellowship.

REFERENCES

1. M. Grazel, *Nature*, 2001, **414**, 338-344.

2. A. H. Khan, U. Thupakula, A. Dalui, S. Maji, A. Debangshi and S. Acharya, *J. Phys. Chem. C*, 2013, **117**, 7934-7939.

3. K. A. Mazzio and C. K. Luscombe, *Chem. Soc. Rev.*, 2015, **44**, 5744-5744.

4. W. Chaikittisilp, K. Ariga and Y. Yamauchi, *J. Mater. Chem. A*, 2013, **1**, 14-19.

5. B. Tian, X. Zheng, T. J. Kempa, Y. Fang, N. Yu, G. Yu, J. Huang and C. M. Lieber, *Nature*, 2007, **449**, 885-889.

6. S. P. Beeby, R. N. Torah, M. J. Tudor, P. Glynne-Jones, T. O'Donnell, C. R. Saha and S. Roy, *J. Micromech. Microeng.*, 2007, **17**, 1257-1265.

7. R. Torah, P. Glynne-Jones, M. Tudor, T. O'Donnell, S. Roy and S. Beeby, *Meas. Sci. Technol.*, 2008, **19**, 125202.

RSC Advances Accepted Manuscript

8. D. Kraemer, B. Poudel, H. -P. Feng, J. C. Caylor, B. Yu, X. Yan, Y. Ma, X. Wang, D. Wang, A. Muto, K. McEnaney, M. Chiesa, Z. Ren and G. Chen, *Nat. Mater.*, 2011, **10**, 532-538.

9. L. E. Bell, *Science*, 2008, **321**, 1457-1461.

10. R. Venkatasubramanian, E. Siivola, T. Colpitts and B. O'Quinn, *Nature*, 2001, **413**, 597-602.

11. Z. L. Wang and J. H. Song, *Science*, 2006, **312**, 242-246.

12. R. A. Whiter, V. Narayan and S. Kar-Narayan, *Adv. Energy Mater.*, 2014, **4**, 1400519.

13. R. Yang, Y. Qin, L. Dai and Z. L. Wang, *Nat. Nanotechnol.*, 2009, **4**, 34-39.

14. X. Wang, J. Song, J. Liu and Z. L. Wang, *Science*, 2007, **316**, 102-105.

15. K. Park, J. H. Son, G. -T. Hwang, C. K. Jeong, J. Ryu, M. Koo, I. Choi, S. H. Lee, M. Byun, Z. L. Wang and K. J. Lee, *Adv. Mater.*, 2014, **26**, 2514-2520.

16. S. Wang, L. Lin and Z. L. Wang, *Nano Lett.*, 2012, **12**, 6339-6346.

17. S. Wang, S. Niu, J. Yang, L. Lin and Z. L. Wang, *ACS Nano*, 2014, **8**, 12004-12013.

18. G. Cheng, Z. -H. Lin, Z. Du and Z. L. Wang, *Adv. Funct. Mater.*, 2014, **24**, 2892-2898.

19. A. Tamang, S. K. Ghosh, S. Garain, M. M. Alam, J. Haeberle, K. Henkel, D. Schmeisser and D. Mandal, *ACS Appl. Mater. Interfaces*, 2015, **7**, 16143-16147.

20. W. Seung, M. K. Gupta, K. Y. Lee, K. -S. Shin, J. -H. Lee, T. Y. Kim, S. Kim, J. Lin, J. H. Kim and S. -W. Kim, *ACS Nano*, 2015, **9**, 3501-3509.

21. X. Li, Y. -H. Wang, C. Zhao and X. Liu, *ACS Appl. Mater. Interfaces*, 2014, **6**, 22004-22012.

RSC Advances Accepted Manuscript

22. Y. Yang, H. Zhang, X. Zhong, F. Yi, R. Yu, Y. Zhang and Z. L. Wang, *ACS Appl. Mater. Interfaces*, 2014, **6**, 3680-3688.

23. J. A. Cross, *Electrostatics: Principles, Problems and Applications*, Adam Hilger, Bristol, 1987.

24. Y. Zheng, L. Cheng, M. Yuan, Z. Wang, L. Zhang, Y. Qin and T. Jing, *Nanoscale*, 2014, **8**, 7842-7846.

25. S. Maji, P. K. Sarkar, L. Aggarwal, S. K. Ghosh, D. Mandal, G. Sheet and S. Acharya, *Phys. Chem. Chem. Phys.*, 2015, **17**, 8159-8165.

26. Y. Zi, S. Niu, J. Wang, Z. Wen, W. Tang and Z. L. Wang, *Nat. Commun.*, 2015, **6**, 8376.

27. R. Gregorio Jr and M. Cestari, *J. Polym. Sci., Part B: Polym. Phys.*, 1994, **32**, 859-870.

TOC:

Triboelectric generator composed of poly(vinylidene fluoride) and polyethylene shows output voltage of ~20 V lighting at least 12 LEDs.

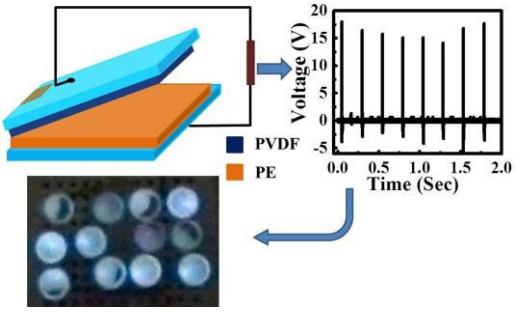

RSC Advances Accepted Manuscript